J|A|C|S ARTICLES

Published on Web 11/24/2010

Encapsulated Energy-Transfer Cassettes with Extremely Well Resolved Fluorescent Outputs

Yuichiro Ueno,[†] Jiney Jose,[†] Aurore Loudet,[†] César Pérez-Bolívar,[‡] Pavel Anzenbacher, Jr.,[‡] and Kevin Burgess*,[†]

Departments of Chemistry, Texas A & M University, Box 30012, College Station, Texas 77841, United States, and Bowling Green State University, Bowling Green, Ohio 43403, United States

Received August 10, 2010; E-mail: burgess@tamu.edu

Abstract: This paper concerns the development of water-compatible fluorescent imaging probes with tunable photonic properties that can be excited at a single wavelength. Bichromophoric cassettes **1a**−**1c** consisting of a BODIPY donor and a cyanine acceptor were prepared using a simple synthetic route, and their photophysical properties were investigated. Upon excitation of the BODIPY moiety at 488 nm the excitation energy is transferred through an acetylene bridge to the cyanine dye acceptor, which emits light at approximately 600, 700, and 800 nm, i.e., with remarkable dispersions. This effect is facilitated by efficient energy transfer that gives a "quasi-Stokes" shift between 86 and 290 nm, opening a huge spectral window for imaging. The emissive properties of the cassettes depend on the energy-transfer (ET) mechanism: the faster the transfer, the more efficient it is. Measurements of rates of ET indicate that a through-*bond* ET takes place in the cassettes **1a** and **1b** that is 2 orders of magnitude faster than the classical through-*space*, Förster ET. In the case of cassette **1c**, however, both mechanisms are possible, and the rate measurements do not allow us to discern between them. Thus, the cassettes **1a**−**1c** are well suited for multiplexing experiments in biotechnological methods that involve a single laser excitation source. However, for widespread application of these probes, their solubility in aqueous media must be improved. Consequently, the probes were encapsulated in calcium phosphate/silicate nanoparticles (diameter ca. 22 nm) that are freely dispersible in water. This encapsulation process resulted in only minor changes in the photophysical properties of the cassettes. The system based on cassette **1a** was chosen to probe how effectively these nanoparticles could be used to deliver the dyes into cells. Encapsulated cassette **1a** permeated Clone 9 rat liver cells, where it localized in the mitochondria and fluoresced through the acceptor part, i.e., red. Overall, this paper reports readily accessible, cyanine-based through-bond ET cassettes that are lypophilic but can be encapsulated to form nanoparticles that disperse freely in water. These particles can be used to enter cells and to label organelles.

Introduction

Fluorescent labels that display high photostability and chemical stability, bright fluorescence, and emission wavelength tunability are important tools in cellular biology.[1,2] Such labels generally allow for high-quality images at lower photon flux, without sacrificing accuracy (low background). If the labels allow channel multiplexing, then that is also an advantage, as it facilitates tracking of several components in a single experiment.[3,4] However, large Stokes' shifts are required to achieve resolutions necessary for multiplexing experiments. These shifts correspond to energies required for reorganization from ground to excited states;[5,6] for most planar, conjugated organic labels, which have relatively small Stokes' shifts (10−20 nm),[7] this parameter is not easily manipulated.[8,9] Thus, multiplexed fluorescent labels for excitation at one wavelength must involve compromise between two opposing physical parameters.[3] If the excitation source is set at the absorption maxima of the dyes used, then all the dyes must have nearly the same absorption maxima, and the limit of the resolution is defined by the Stokes' shifts of the dyes. Conversely, if the dyes are chosen for their diverse fluorescence emission maxima, then the UV absorption maxima of some of the dyes will not correspond to the excitation wavelength, these dyes will absorb less light, and they will fluoresce less brightly.

[†] Texas A & M University.
[‡] Bowling Green State University.

(1) Sauer, M.; Hofkens, J.; Enderlein, J. *Handbook of Fluorescence Spectroscopy and Imaging: From Ensemble to Single Molecules*; Wiley-VCH: Weinheim, 2010.
(2) Sabnis, R. W. *Handbook of Biological Dyes and Stains. Synthesis and Industrial Applications*; Wiley & Sons: Hoboken, NJ, 2010.
(3) Levenson, R. M.; Mansfield, J. R. *Cytometry* **2006**, *69*, 748–758.
(4) Haney, S. A. *High Content Screening: Science, Techniques and Applications*; Wiley-Interscience: Hoboken, NJ, 2008.
(5) Delmotte, C.; Delmas, A. *Bioorg. Med. Chem. Lett.* **1999**, *9*, 2989–2994.
(6) Taylor, D. L.; Haskins, J. R.; Giuliano, K. A. *High Content Screening: A Powerful Approach to Systems Cell Biology and Drug Discovery*; Humana Press: Totowa, NJ, 2007; Vol. 356.
(7) Montalti, M.; Credi, A.; Prodi, L.; Gandolfi, M. T. *Handbook of Photochemistry*, 3rd ed.; CRC Press-Taylor & Francis: Boca Raton, FL, 2006.
(8) Wang, L.; Tan, W. *Nano Lett.* **2006**, *6*, 84–88.
(9) Lakowicz, J. R. *Principles of Fluorescence Spectroscopy*, 3rd ed.; Springer: New York, 2006.

Many applications in bioimaging require probes that are compatible with aqueous media. Incorporation of water-solubilizing groups in labels is a challenge[10] and presents problems during purification,[5] especially since even small amounts of fluorescent impurities may skew the data obtained in imaging experiments. Furthermore, water-solubilizing groups attached to fluors often result in decreased fluorescence intensities due to nonradiative decay processes facilitated by solvation sphere rearrangement in the excited state.[11,12] Finally, if these obstacles are overcome, the resulting labels may be highly polar; this tends to impart an increased affinity for cytoplasm, making the probes less useful for imaging of other cellular compartments.

Here we present a rational design of fluorescent labels that allows tuning of fluorescent outputs through a wide emission window via cassettes composed of donor and acceptor chromophores.[8,11,13,14] Specifically, this paper describes cassettes that work via excitation of a BODIPY-based[15−18] donor with blue light (e.g., 488 nm) followed by fast energy transfer (ET) to variable cyanine-based[19,20] acceptors, which then emit red light. Three cassettes were prepared, **1a**−**1c** (Scheme 1). The wavelength of the emitted light depends on the structure of the acceptor and varies from 590 to 794 nm. While the Stokes' shift of the donor is short (~20 nm), the red shift in the cassettes is between 86 and 290 nm; this dispersion is greater than any other achieved in cassettes generated in these laboratories.[21−29] These probes are relatively easy to make, partly because they are lipophilic, but they have poor water solubilities. To obviate this issue, the cassettes were encapsulated in calcium phosphate/silicate nanoparticles that are freely dispersed in water. Experiments are described to elucidate how these particles can be used as delivery agents wherein the dye-containing particles become localized within the cells.

Scheme 1. Syntheses of the Through-Bond Energy-Transfer Cassettes **1a**−**1c**

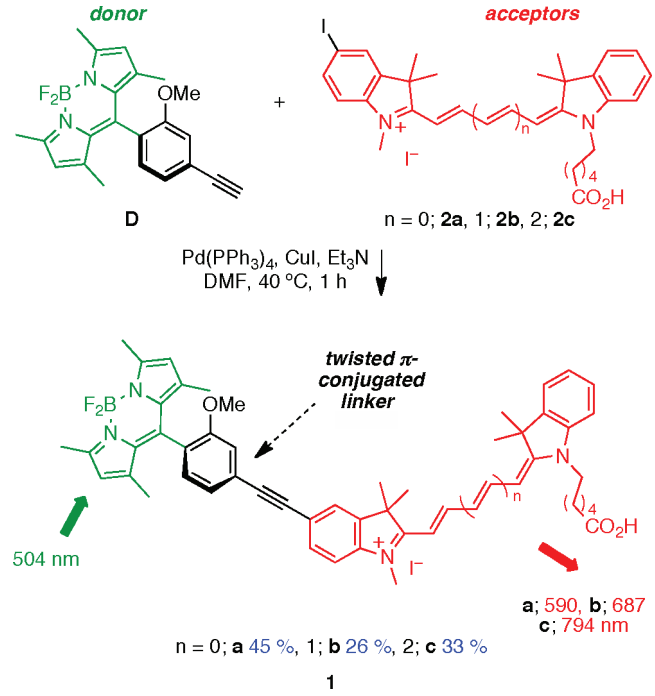

Results and Discussion

Syntheses and Spectroscopic Properties of the Cassettes. Cassettes **1a**−**1c** were prepared by cross-coupling the readily available donor fragment **D** with the iodine-functionalized cyanine dyes **2a**−**2c** (Scheme 1 and Supporting Information). These materials were easily purified via flash chromatography because they are lipophilic and colored.

Spectroscopic data for the cassettes **1** are presented in Figure 1 and Table 1. Figure 1a shows the absorbance spectra; these resemble the summation of components from the donor and acceptor fragments. When the cassettes are excited at 504 nm (the donor), **1a** and **1b** emit predominantly from their acceptor fragments; only about 10% of the fluorescence "leaks" from the donor part. Leakage from the donor is prevalent in the fluorescent spectra of **1c** under the same conditions. Quantitatively, this parameter is reflected by the energy-transfer efficiencies (ETEs; $\{\Phi_d/\Phi_a\} \times 100\%$)[29] of these cassettes (**1a** and **1b**, >88%; **1c**, 43%).

We speculate that the difference in quantum yields for the three cassettes after encapsulation is due to the orientation of the cassettes within the particles. In the case of cassette **1a** (Cy3 cassette), the fluor is well encapsulated and devoid of any π-stacking; hence, its quantum yield is high. However, **1b** and **1c** may be oriented in ways that favor more π-stacking, resulting in lower quantum yields.

Ultrafast Spectroscopy Measurements. Ethynylene linkers were incorporated in cassettes **1a**−**1c** to facilitate donor-to-acceptor ET through *bonds*,[30] though through-*space* ET is also plausible. Femtosecond transient spectroscopy was performed to compare actual rates of ET in these systems to ones calculated

(10) Romieu, A.; Brossard, D.; Hamon, M.; Outaabout, H.; Portal, C.; Renard, P.-Y. *Bioconjugate Chem.* **2008**, *19*, 279–289.
(11) Förster, T. *Naturwissenschaften* **1946**, *6*, 166–175.
(12) Laia, C. A. T.; Costa, S. M. B. *Chem. Phys. Lett.* **1998**, *285*, 385–390.
(13) Zhu, L.; Soper, S. A. *Rev. Fluoresc.* **2006**, *3*, 525–574.
(14) Lakowicz, J. R. *Principles of Fluorescence Spectroscopy*, 2nd ed.; Kluwer Academic/Plenum Publishers: New York, 1999.
(15) Loudet, A.; Burgess, K. In *Handbook of Porphyrin Science: With Applications to Chemistry, Physics, Materials Science, Engineering, Biology and Medicine*; Kadish, K., Smith, K., Guilard, R., Eds.; World Scientific: Singapore, 2010; p 203.
(16) Ulrich, G.; Ziessel, R.; Harriman, A. *Angew. Chem., Int. Ed.* **2008**, *47*, 1184–1201.
(17) Ziessel, R.; Ulrich, G.; Harriman, A. *New J. Chem.* **2007**, *31*, 496–501.
(18) Loudet, A.; Burgess, K. *Chem. Rev.* **2007**, *107*, 4891–4832.
(19) Mishra, A.; Behera, R. K.; Behera, P. K.; Mishra, B. K.; Behera, G. B. *Chem. Rev.* **2000**, *100*, 1973–2011.
(20) Ozhalici-Unal, H.; Pow, C. L.; Marks, S. A.; Jesper, L. D.; Silva, G. L.; Shank, N. I.; Jones, E. W.; Burnette, J. M., III; Berget, P. B.; Armitage, B. A. *J. Am. Chem. Soc.* **2008**, *130*, 12620–12621.
(21) Burgess, K.; Burghart, A.; Chen, J.; Wan, C.-W. *Proc. SPIE−Int. Soc. Opt. Eng.* **2000**, *3926*, 95–105.
(22) Burghart, A.; Thoresen, L. H.; Chen, J.; Burgess, K.; Bergstrom, F.; Johansson, L. B.-A. *Chem. Commun.* **2000**, 2203–2204.
(23) Jiao, G.-S.; Thoresen Lars, H.; Burgess, K. *J. Am. Chem. Soc.* **2003**, *125*, 14668–14669.
(24) Wan, C.-W.; Burghart, A.; Chen, J.; Bergstroem, F.; Johansson, L. B. A.; Wolford, M. F.; Kim, T. G.; Topp, M. R.; Hochstrasser, R. M.; Burgess, K. *Chem.−Eur. J.* **2003**, *9*, 4430–4441.
(25) Burgess, K. (The Texas A&M University System). U.S. Patent 0032120 A1, 2005.
(26) Bandichhor, R.; Petrescu, A. D.; Vespa, A.; Kier, A. B.; Schroeder, F.; Burgess, K. *J. Am. Chem. Soc.* **2006**, *128*, 10688–10689.
(27) Kim, T. G.; Castro, J. C.; Loudet, A.; Jiao, J. G. S.; Hochstrasser, R. M.; Burgess, K.; Topp, M. R. *J. Phys. Chem. A* **2006**, *110*, 20–27.
(28) Jose, J.; Ueno, Y.; Wu, L.; Loudet, A.; Chen, H.-Y.; Son, D. H.; Burgess, K. *Chem. Commun.* **2009**, submitted.
(29) Wu, L.; Loudet, A.; Barhoumi, R.; Burghardt, R. C.; Burgess, K. *J. Am. Chem. Soc.* **2009**, *131*, 9156–9157.
(30) Polyansky, D. E.; Danilov, E. O.; Voskresensky, S. V.; Rodgers, M. A. J.; Neckers, D. C. *J. Am. Chem. Soc.* **2005**, *127*, 13452–13453.

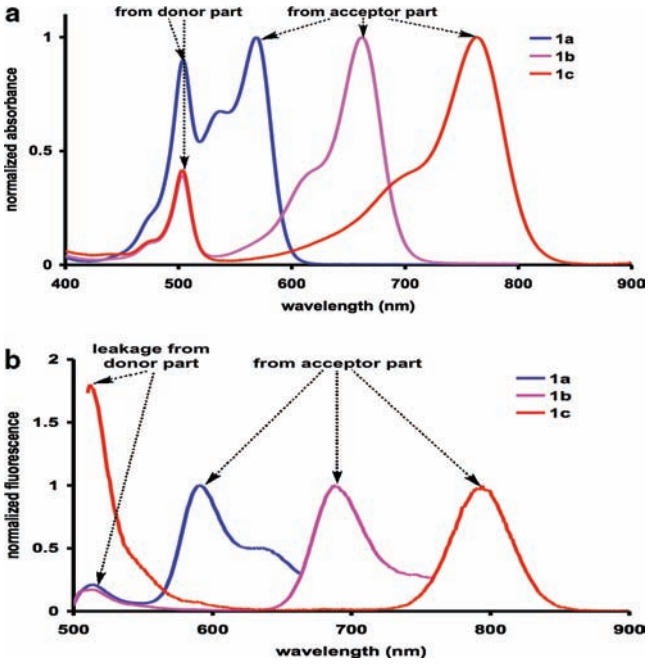

Figure 1. Normalized (a) absorbance and (b) fluorescence spectra of the cassettes in EtOH (at 10^{-6} and 10^{-7} M for absorbance and fluorescence measurements, respectively).

Table 1. Photophysical Properties of Cassettes

	λ_{abs} (nm)	λ_{em} (nm)	Φ_d[a]	Φ_a[b]	ETE (%)
			In EtOH		
1a	504, 569	519, 590	0.20±0.01	0.22±0.02	90
1b	504, 662	519, 687	0.35±0.02	0.40±0.03	87
1c	504, 763	519, 794	0.11	–[c]	43[d]
			Nanoparticles in pH 7.4 Phosphate Buffer		
1a	504, 568	519, 592	0.26±0.01	0.29±0.02	88
1b	504, 659	519, 687	0.063	0.071	89
1c	504, 764	519, 793	0.053	–[c]	41[d]

[a] Quantum yield of acceptor when excited at donor relative to rhodamine 6G ($\Phi = 0.92$ in EtOH). [b] Quantum yield of acceptor when excited at acceptor relative to rhodamine 101 for **1a** ($\Phi = 1.0$ in EtOH) and Nile Blue for **1b** ($\Phi = 0.27$ in EtOH). [c] No appropriate standard due to range of wavelengths. [d] See Supporting Information for calculation. Quantum yields were measured three times and averaged, and they were corroborated using the absolute fluorescence quantum yield measurements. ETE, energy transfer efficiency, calculated as $(\Phi_d/\Phi_a) \times 100\%$.

for transfer through *space* (fluorescence resonance energy transfer, FRET). As a control, *intermolecular* ET between the donor **D** in ethanol and an equimolar (3.1×10^{-6} M) concentration of the non-iodinated analogues of the acceptors (**2a**, Cy3) was also studied. Energy transfer did occur under these conditions, at a rate of 1.85×10^9 s^{-1}.

Energy transfer rates were measured for the cassettes **1a**−**1c** (at the concentration of 3.1×10^{-6} M) and compared with the

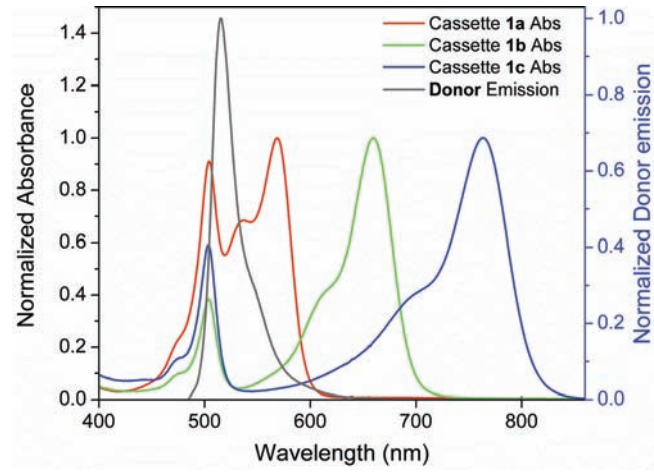

Figure 2. Spectral overlap of BODIPY donor emission (black line) and cassette absorption (**1a**, red line; **1b**, green line; **1c**, blue line) ensures resonance energy transfer.

rates calculated for through-*space* ET using the Förster model (Table 2). From the perspective of the resonance energy transfer (RET) theory, the overlap integral J for the emission of the donor (common for the three cassettes) and the absorption of the indocyanine acceptor (Figure 2) show a stepwise decrease **1a** > **1b** > **1c**, while the Förster radius (R_0) increases. Following the Förster model, the calculated theoretical value for the RET decreases from 8.59×10^9 for **1a** to 1.88×10^9 for **1b** and 1.39×10^9 for **1c** (Table 2). Consequently, the Förster ET rate calculated for cassette **1a**, for instance, was approximately 4 times faster than the observed rate for the intermolecular transfer in the control described above.

Observed ET rates for cassettes **1a** and **1b** were 2 orders of magnitude higher than the rates predicted for the Förster model. Specifically, the rates for **1a** and **1b** are 56 and 67 times faster than the ones calculated for through-space ET (Table 2). These data suggest a dramatic effect of the donor−acceptor communication through the phenylethyne bridge.

Cassette **1c** shows an ET rate equal (within 10% error) to the through-*space* ET rate following the Förster model. This suggests that in **1c** the RET proceeds through-*space* or in a mixed through-*space* and through-*bond* mechanism. Overall, the measured rates suggest the efficiency decreases from 90 to 87 and 43% for **1a**, **1b**, and **1c**, respectively.

On a picosecond time scale, ET was observed by following the concerted kinetics of the donor-stimulated emission decay after the excitation and the population of the acceptor excited state following the bleaching of the donor. After the energy is transferred, the acceptor decays at its usual time scale, i.e., as if excited directly. For example, excitation of cassette **1a** at the donor (420 nm) by a femtosecond laser pulse is followed by the decay of a singlet state, which is complete within 2.1 ps and is accompanied by the population of an acceptor excited

Table 2. Energy-Transfer Data Calculated and Recorded Using Time-Resolved Fluorescence Spectroscopy and Femtosecond Transient Spectroscopy in Ethanol at 22 °C

cassette	transfer rate measured (s^{-1})	Förster radius calcd R_0 (Å)	overlap integral J (M^{-1} cm^3 nm^4)	transfer rate calcd (s^{-1})[a]	measured ET efficiency (%)	donor decay (ps)	acceptor raise (ps)	acceptor decay (ps)
1a	4.85×10^{11}	129	3.47×10^{17}	8.59×10^9	90	2.06	2.18	352
1b	1.26×10^{11}	100	7.61×10^{16}	1.88×10^9	87	7.96	9.55	~1000
1c	1.26×10^9	94	5.14×10^{16}	1.39×10^9	43	794	ND[b]	719

[a] Transfer rate for the Förster through-*space* ET was calculated using r (donor−acceptor distance), determined as an average center-to-center distance using $k_T(r) = R_0^6/\tau_D$, $\chi^2 = 2/3$, r^6 formula, and $r = 66.41$ Å. [b] Relatively fast population of the acceptor singlet excited state occurred due to the direct pumping of the acceptor absorption by the laser (**1c**, $\varepsilon_{420} = 9800$ M^{-1} cm^{-1}).

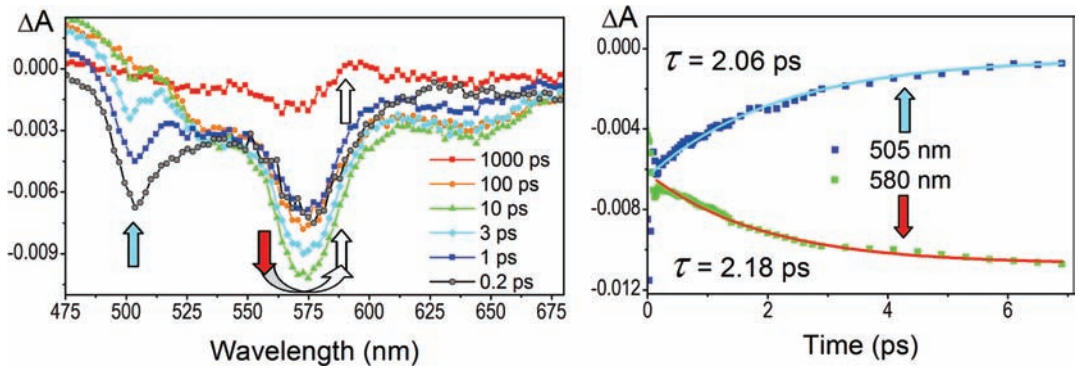

Figure 3. (Left) Transient absorption spectra of the cassette **1a** showing a concerted depletion of the stimulated emission donor maximum at 505 nm (blue arrow) and raise of the acceptor maxima at 580 nm (red arrow), followed by acceptor relaxation within 350 ps. (Right) Kinetic profiles of the donor decay (2.06 ps) and acceptor raise (2.18 ps) reflect the concerted process.

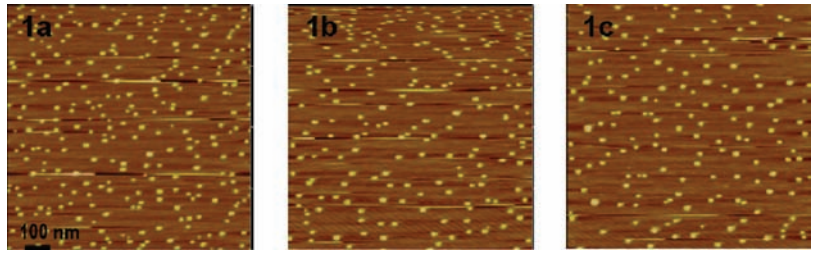

Figure 4. Atomic force microscopy images of cassettes encapsulated in calcium phosphate nanoparticles. Average particle size, 22 nm.

state with 2.2 ps raise time. Thereafter, the acceptor decays with a fluorescence lifetime of 352 ps by emitting with a λ_{max} of 600 nm (Figure 3). Similarly, exciting cassette **1b** at 420 nm results in singlet-state population of the BODIPY donor, decay within 8.0 ps, and then complete population of the acceptor excited state after 9.6 ps; the acceptor singlet excited state decays with a fluorescence lifetime of ~1 ns (λ_{max} = 680 nm). In contrast to the other two cassettes, the donor of **1c** decays slowly (within 800 ps), which suggests that the excited state of the donor is not being depopulated by a strongly coupled acceptor as it is in the cassettes **1a** and **1b**, and the ET is less efficient. Through-*space* RET is still operational in the cassette **1c** since the donor alone decays with a lifetime of 4 ns, which is comparable to the 800 ps rate in the cassette.

The following conclusions can be drawn from the measurement of ET rates. First, a significantly more efficient pathway for donor−acceptor communication exists for cassettes **1a** and **1b** compared to that in **1c**. Aryl−ethynyl−aryl moieties display a strong electronic coupling,[30] and this suggests that the ET takes place through the bridge. The efficiency and rate of the ET processes in **1a** and **1b** are a strong indication of an exciton hopping mechanism.[31−34] Cassette **1c** transfers energy at a rate that can be rationalized using the Förster through-*space* model.

Encapsulation of the Dyes in Calcium Phosphate/Silicate. Cassettes **1a**−**1c** are not water-soluble, but we show here that they can be encapsulated in calcium phosphate to form nanoparticles. With respect to biotechnological applications, calcium phosphate is an excellent matrix for nanoparticle encapsulation because (i) moderate concentrations of Ca^{2+} ions are not toxic to cells; (ii) it is not toxic *in vivo* (found in human bone and teeth); (iii) it is claimed that calcium phosphate dissolves below pH 5.5 to liberate the cargo but is stable at 7.4;[35] (iv) particles of this matrix disperse freely in aqueous media; and (v) the surface of these particles can be functionalized.[36,37] Adair and co-workers have shown that spherical, ca. 18 nm diameter calcium phosphate nanoparticles can be formed with citrate-derived surface carboxylate groups and fluorescent dye cargoes.[38] They have investigated these particles for imaging in cells and *in vivo*.[39−43]

In our work, calcium phosphate/silicate nanoparticles encapsulating cassettes **1a**−**1c** were prepared via Adair's procedure[38] except that a longer reaction time was used (24 h, not 5 min), the particles were purified via medium-pressure rather than high-pressure liquid chromatography, and finally a dialysis step was performed to transfer the particles from an ethanolic to an aqueous medium. Figure 4 shows atomic force microscopy

(31) Davis, W. B.; Svec, W. A.; Ratner, M. A.; Wasielewski, M. R. *Nature* **1998**, *396*, 60–63.
(32) Kim, D.; Osuka, A. *Acc. Chem. Res.* **2004**, *37*, 735–745.
(33) Montes, V. A.; Perez-Bolivar, C.; Estrada, L. A.; Shinar, J.; Anzenbacher, P., Jr. *J. Am. Chem. Soc.* **2007**, *129*, 12598–12599.
(34) Montes, V. A.; Perez-Bolivar, C.; Agarwal, N.; Shinar, J.; Anzenbacher, P., Jr. *J. Am. Chem. Soc.* **2006**, *128*, 12436–12438.
(35) Bisht, S.; Bhakta, G.; Mitra, S.; Maitra, A. *Int. J. Pharm.* **2005**, *288*, 157–168.
(36) Altinoglu, E. I.; Russin, T. J.; Kaiser, J. M.; Barth, B. M.; Eklund, P. C.; Kester, M.; Adair, J. H. *ACS Nano* **2008**, *2*, 2075–2084.
(37) Morgan, T. T.; Muddana, H. S.; Altinoglu, E. I.; Rouse, S. M.; Tabakovic, A.; Tabouillot, T.; Russin, T. J.; Shanmugavelandy, S. S.; Butler, P. J.; Eklund, P. C.; Yun, J. K.; Kester, M.; Adair, J. H. *Nano Lett.* **2008**, *8*, 4108–4115.
(38) Altınoğlu, E. I.; Russin, T. J.; Kaiser, J. M.; Barth, B. M.; Eklund, P. C.; Kester, M.; Adair, J. H. *ACS Nano* **2008**, 2075–2086.
(39) Morgan, T. T.; Muddana, H. S.; lu, E. I. A.; Rouse, S. M.; Tabakovic, A.; Tabouillot, T.; Russin, T. J.; Shanmugavelandy, S. S.; Butler, P. J.; Eklund, P. C.; Yun, J. K.; Kester, M.; Adair, J. H. *Nano Lett.* **2008**, *8*, 4108–4115.
(40) Muddana, H. S.; Morgan, T. T.; Adair, J. H.; Butler, P. J. *Nano Lett.* **2009**, 1559–1566.
(41) Kester, M.; Heakal, Y.; Fox, T.; Sharma, A.; Robertson, G. P.; Morgan, T. T.; Altinoglu, E. I.; Tabakovic, A.; Parette, M. R.; Rouse, S.; Ruiz-Velasco, V.; Adair, J. H. *Nano Lett.* **2008**, *8*, 4116–4121.
(42) Gupta, R.; Mishra, P.; Mittal, A. *J. Nanosci. Nanotechnol.* **2009**, *9*, 2607–2615.
(43) Glowka, E.; Lamprecht, A.; Ubrich, N.; Maincent, P.; Lulek, J.; Coulon, J.; Leroy, P. *Nanotechnology* **2006**, *17*, 2546–2552.

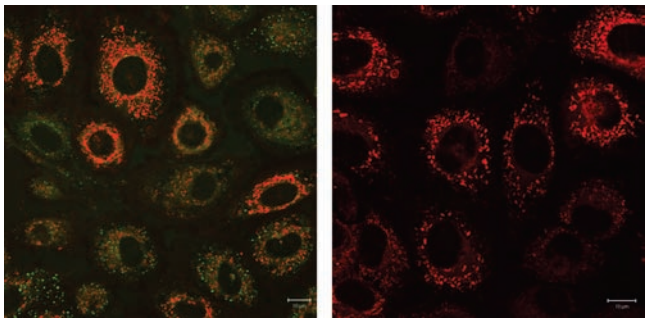

Figure 5. Fluorescence images of cassette **1a** (left) and **1a-CaNP** (right) in normal rat liver cells (Clone 9). Scale bar is 10 μm.

images of the particles formed from the cassettes **1**; these are quite uniform, with diameters around 22 nm.

Spectroscopically, encapsulated cassettes **1a**−**1c** had absorption and fluorescent spectra that are almost identical to those of the free cassettes in EtOH (see Table 1). The quantum yield of encapsulated **1a -CaNP** increased about 30% relative to the free dye in EtOH, but for **1b-CaNP** and **1c-CaNP** it decreased by 5- and 2-fold respectively, which is satisfactory for some applications. Throughout, the ETEs were essentially unchanged.

Permeation of the Particles into Clone 9 Rat Liver Cells. Cassette **1a** and **1a-CaNPs** were imported in Clone 9 cells at 37 °C to study their subcellular localization. Cassette **1a** was observed in different organelles: the mitochondria, the lysosomes, the endoplasmic reticulum (ER), and the cytoplasm. Interestingly, the emission output observed was dependent on the subcellular compartment. Thus, in the mitochondria, perfect ET was observed; i.e., only emission from the cyanine was seen, hence the probes fluoresced red. Diffuse *green* fluorescence was observed in the cytoplasm and ER and in some bright punctates (lysosomes); the green fluorescence is indicative of emission from the donor part. Conversely, **1a-CaNPs** localized only in the mitochondria, and sole emission from the cyanine part was observed; i.e., the dyes fluoresced red (Figure 5). When the cells were treated with **1a-CaNPs** at 4 °C, no fluorescent signal could be observed after 2 h incubation, indicating that the nanoparticles may enter via endocytosis.

Conclusions

The research described here represents the first report of coupling BODIPY-based donors with *cyanine* acceptors in ways that facilitate energy transfer through *bonds*. The dispersion of fluorescence emissions from these cassettes is greater than any others prepared by us or, to the best of our knowledge, by others. The observed ET rates for cassettes **1a** and **1b** are significantly faster than for dipole−dipole coupling in a through-*space* manner, indicating transfer through bonds is indeed occurring. Overall, they are excellent tools for fluorescence multiplexing in biotechnology.

Syntheses of such cassettes are straightforward because they are lipophilic. The idea of using water-dispersible nanoparticles to bring lipophilic *cassettes* into aqueous media, thereby circumventing syntheses of water-soluble materials, is novel and has the potential to be applied to other donor−acceptor systems where water-soluble modifications would be hard to make. The absorbance and emission maxima of the *cassettes* and the extent of donor−acceptor energy transfer (ETE) remained significantly unchanged after encapsulation into nanoparticles. Conversely, and surprisingly, the fluorescence quantum yields of the three systems studied in this paper were significantly affected. Thus, the fluorescence quantum yield for **1a-CaNPs** increased by about 30% relative to the free dye in EtOH, while for **1b-CaNPs** and **1c-CaNPs** it decreased by 5- and 2-fold, respectively. Nanoparticles encapsulating these cassettes may have applications for intracellular imaging and for observation of parallel macroscopic events *in vivo*, e.g., as labels for targeting different cancer forms simultaneously, and allow specific targeting of organelles. Other applications beyond organelle targeting in cells can now be envisaged.

Acknowledgment. The TAMU/LBMS-Applications Laboratory directed by Dr. Shane Tichy assisted with mass spectrometry, and Prof. A. Tarnovsky and his staff helped with acquiring the transient spectra. Support for this work was provided by the National Institutes of Health (GM72041) and by The Robert A. Welch Foundation (A1121).

Supporting Information Available: Detailed procedure for the synthesis of the calcium phosphate nanoparticles, their physical properties, rate of energy transfer calculations, and cell imaging. This material is available free of charge via the Internet at http://pubs.acs.org.

JA107193J